DALTON
FULL PAPER

Orotate complexes of rhodium(I) and iridium(I): effect of coligand, counter ion, and solvent of crystallisation on association *via* complementary hydrogen bonding

Stuart L. James, D. Michael P. Mingos,*,† Xingling Xu, Andrew J. P. White and David J. Williams

Department of Chemistry, Imperial College of Science, Technology and Medicine, South Kensington, London, UK SW7 2AY

The new complexes $[NEt_3H][M(HL)(cod)]$ (M = Rh **1** or Ir **2**; H_3L = 2,6-dioxo-1,2,3,6-tetrahydropyrimidine-4-carboxylic acid, orotic acid; cod = cycloocta-1,5-diene) have been prepared by the reaction between $[M_2Cl_2(cod)_2]$ and orotic acid in dichloromethane in the presence of Ag_2O and NEt_3. They crystallise as dichloromethane adducts **1**·CH_2Cl_2 and **2**·CH_2Cl_2 from dichloromethane–hexane solutions. These isomorphous structures contain doubly hydrogen-bonded dimers, with additional hydrogen bonding to NEt_3H^+ cations and bridging CH_2Cl_2 molecules to form tapes. The use of NBu^n_4OH instead of NEt_3 gave the related complex $[NBu^n_4][Rh(HL)(cod)]$ **1′** which has an innocent cation not capable of forming strong hydrogen bonds and in contrast to **1** exists as discrete doubly hydrogen-bonded dimers. Complex **1′** cocrystallises with 2,6-diaminopyridine (dap) *via* complementary triple hydrogen bonds to give $[NBu^n_4][Rh(HL)(cod)]$·dap·CH_2Cl_2 **3**. Complex **3** exhibits an extended sheet structure of associated [2 + 2] units, with layers of NBu^n_4 cations separating the sheets. These structural data together with those reported previously for platinum orotate complexes suggest that the steric requirements of the other ligands co-ordinated to the metal are important in influencing their hydrogen-bonding abilities. The solvent of crystallisation, the hydrogen-bonding propensity of the coligand and the nature of the counter ion also determine the type of association in the solid state.

Hydrogen-bonding interactions have been used extensively in the development of supramolecular chemistry.[1] The incorporation of metals into supramolecular systems has recently attracted some attention because it generates the possibility of introducing the well developed redox, optical and magnetic properties of transition metals into these systems. Our approach and that of others in this area has been to prepare complexes of ligands which possess both a metal co-ordination site and a domain containing combinations of hydrogen bond acceptors (A) and donors (D).[2] Through the judicious choice of complementary hydrogen-bonding components (and cocrystallised bases) dimers, tapes and sheets have been generated in the solid state. The presence of metals in these systems introduces many additional potential variables which remain to be explored. These include the charge on the complex, the nature of the coligands and the counter ions, which themselves may have the ability to take part in hydrogen bonding, or may simply occupy cavities in the crystal lattice. Earlier studies on orotate complexes (orotic acid = 2,6-dioxo-1,2,3,6-tetrahydropyrimidine-4-carboxylic acid, H_3L) of nickel, copper, zinc,[3] palladium and platinum[4] suggested that they are a suitable class of compounds for exploring these variables. Orotate complexes are particularly attractive since the ADA hydrogen-bonding motif recognises at a molecular level complementary DAD bases. We now report on the synthesis and crystal structures of anionic orotate complexes of rhodium(I) and iridium(I) with the cod (cycloocta-1,5-diene) coligand, both with and without hydrogen-bonding counter ions, and a cocrystal formed by complementary hydrogen-bonding interactions with 2,6-diaminopyridine.

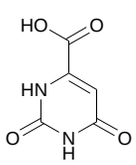

H_3L

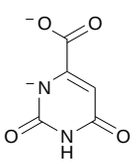

HL^{2-}

† E-Mail: d.mingos@ic.ac.uk

Results and Discussion

Complexes $[NEt_3H][M(HL)(cod)]$ (M = Rh 1 or Ir 2) and $[NBu^n_4][Rh(HL)(cod)]$ 1′

The synthesis of rhodium and iridium orotate complexes was based on the method employed for platinum and palladium complexes.[4a] The reaction between $[M_2Cl_2(cod)_2]$ (M = Rh or Ir) and orotic acid in CH_2Cl_2 in the presence of triethylamine and silver oxide resulted in yellow (Rh) or orange (Ir) solutions, and filtration and slow diffusion of hexane into the filtrate gave crystals which analysed satisfactorily for $[NEt_3H][M(HL)(cod)]$·CH_2Cl_2 (M = Rh **1** or Ir **2**) (see Scheme 1). Infrared spectroscopic data indicated co-ordination to the metal by the orotate ligand. In particular, the carbonyl stretching frequencies at 1650 and 1631 cm^{-1} of **1** were distinctly shifted from those of free orotic acid (1706 and 1666 cm^{-1}) and occurred at similar frequencies to those reported previously for orotate complexes.[3,4] The ^1H NMR spectra in $CDCl_3$ or $(CD_3)_2SO$ indicated the presence of the orotate ligand (alkenyl and N–H resonances), in addition to co-ordinated cod, cocrystallised CH_2Cl_2 and the NEt_3H^+ cation. In order to remove the potential cation–anion hydrogen-bonding complications introduced by the NEt_3H^+ cation we also made the complex $[NBu^n_4][Rh(HL)(cod)]$ **1′** by a modification of the above procedure; NBu^n_4OH was used as a base in place of NEt_3. All analytical and spectroscopic data for complex **1′** were consistent with its formulation. In order to confirm their structures and define the specific hydrogen-bonding modes which are present in the solid state, crystal structure determinations were conducted on the rhodium and iridium complexes **1**, **2** and **1′**.

Crystal structure determinations of complexes 1, 2 and 1′

The structures of the new compounds were confirmed by single-crystal structural analyses. Crystals of **1** and **2** proved to be isomorphous, Fig. 1. The metal co-ordination geometries are distorted square planar with the interligand angles lying in the ranges 80.3(2) to 100.8(3) and 170.2(3) to 176.6(3)° in **1** (M = Rh) and 79.7(2) to 101.5(3) and 169.9(3) to 177.5(3)° in **2** (M = Ir), Table 1. The orotate ligand adopts a conventional *N*,*O* co-ordination mode as observed previously in other d^8 complexes.[4] The comparable bond distances for the two complexes do not differ significantly, the metal–nitrogen distances being in each case slightly longer than those to oxygen. There is a small torsional twist (*ca*. 5°) between the co-ordination planes of the two chelating ligands, if the co-ordination points of the cyclooctadiene ligands are taken to be the centres of the two C=C double bonds.

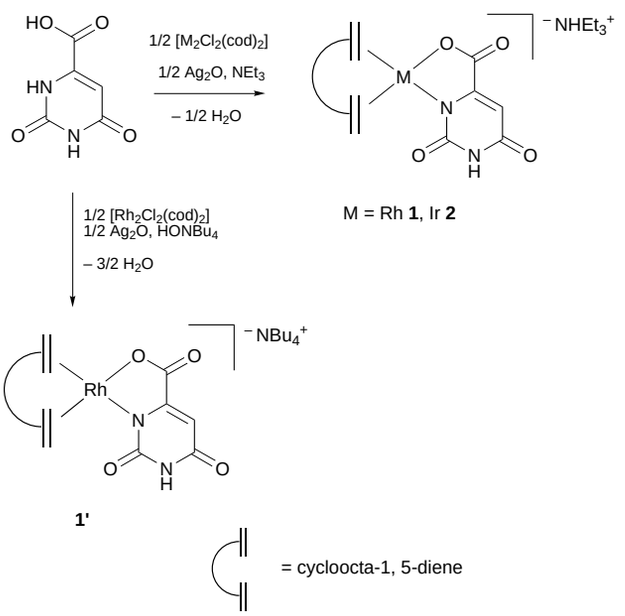

Scheme 1 Synthesis of rhodium and iridium orotate complexes **1**, **2** and **1′**

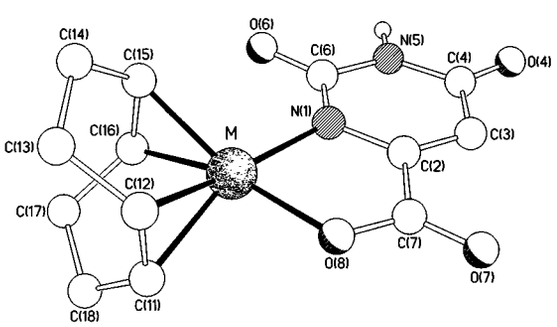

Fig. 1 Molecular structure of the anion in $[NEt_3H][M(HL)(cod)]\cdot CH_2Cl_2$ (M = Rh **1** or Ir **2**) and $[NBu^n_4][Rh(HL)(cod)]$ **1′**

The DAD hydrogen-bonding function on the surface of the orotate complex is not capable of forming triple and complementary hydrogen bonds with like anions and two of the groups are used to form DA : AD dimer pairs between the amide N–H group [N(5)] of one molecule and the adjacent ring carbonyl oxygen atom [O(6)] of a C_2 related counterpart and *vice versa* (linkage *a* in Fig. 2). This arrangement gives rise to eight-membered rings that can be described as $R_2^2(8)$ in Etter's notation.[5] Dimer pairs are linked to their C_i related neighbours *via* weak C–H · · · O hydrogen bonds from the interposed dichloromethane solvent molecules to the two carboxylate oxygen atoms in the orotate ligand (labelled *c* and *d* in Fig. 2) to form sinuous tapes that extend in the crystallographic [101] direction. The remaining orotate acceptor site, O(4), is hydrogen bonded to the N–H centre of the triethylammonium cation (bond *b* in Fig. 2).

The corresponding rhodium NBu^n_4 salt **1′** crystallises free of CH_2Cl_2 molecules although it was crystallised from this solvent. The co-ordination geometry of the [Rh(HL)(cod)] anion does not differ significantly from that observed in **1**, though the twist between the co-ordination planes is reduced to *ca*. 2° (see Table 1). Pairs of C_2 related anions are again linked in a DA : AD

Table 1 Selected bond lengths (Å) and angles (°) for complexes **1**, **2**, **1′** and **3***

	1	**2**	**1′**	**3**
M–N(1)	2.111(5)	2.102(6)	2.089(6)	2.097(5)
M–O(8)	2.053(6)	2.055(6)	2.054(5)	2.056(5)
M–X1	2.001(7)	1.994(8)	1.997(9)	1.999(8)
M–X2	2.006(7)	1.987(8)	2.008(9)	1.983(8)
N(1)–M–O(8)	80.3(2)	79.7(2)	79.9(2)	79.8(2)
N(1)–M–X2	100.8(3)	101.5(3)	101.5(4)	100.2(3)
O(8)–M–X1	91.0(3)	91.1(3)	91.0(4)	91.6(3)
X1–M–X2	88.2(3)	87.9(3)	87.6(4)	88.4(4)
N(1)–M–X1	170.2(3)	169.9(3)	170.9(4)	171.4(3)
O(8)–M–X2	176.6(3)	177.5(3)	177.8(4)	176.3(3)

* X1 = Centre of C(11)–C(12) bond, X2 = centre of C(15)–C(16) bond.

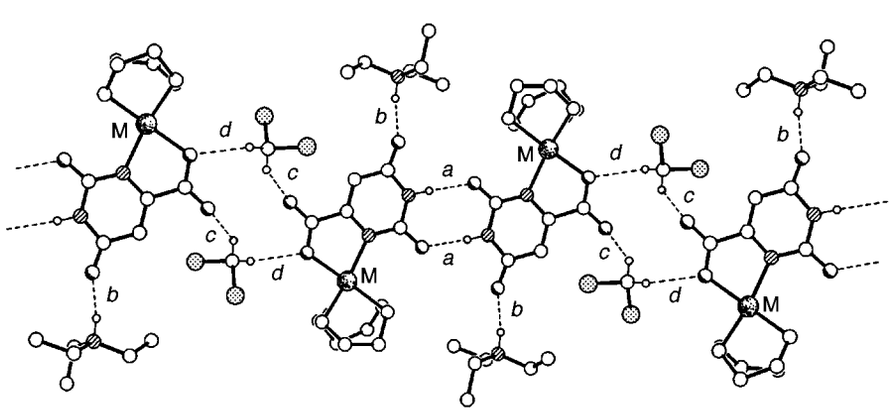

Fig. 2 Part of one of the hydrogen-bonded tapes of molecules present in the structure of $[NEt_3H][M(HL)(cod)]\cdot CH_2Cl_2$ (M = Rh **1** or Ir **2**). Hydrogen-bonding geometries, X · · · O, H · · · O distances (Å) and X–H · · · O angles (°): for **1**, *a*, 2.86(1), 1.97, 170; *b*, 2.69(1), 1.84, 157; *c*, 3.24(1), 2.38, 149; *d*, 3.29(1), 2.40, 154; for **2**, *a*, 2.84(1), 1.94, 178; *b*, 2.70(1), 1.81, 167; *c*, 3.22(1), 2.40, 144; *d*, 3.24(1), 2.39, 148

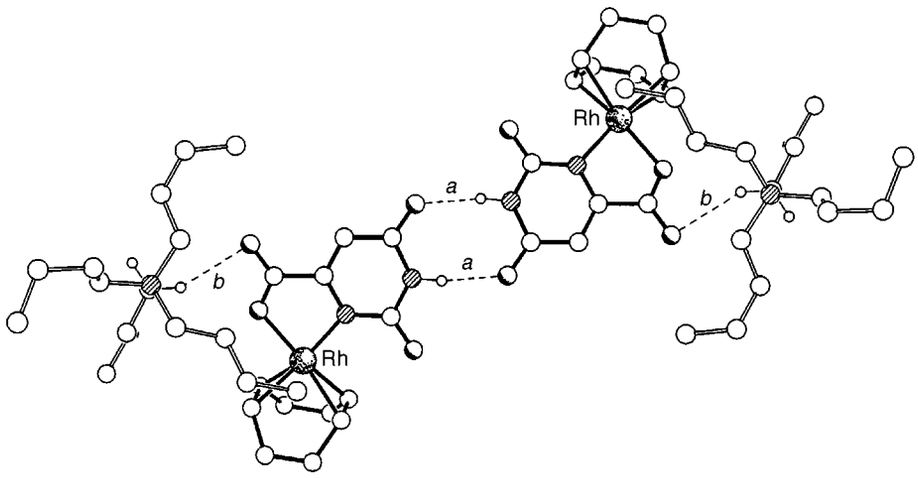

Fig. 3 The AD : DA dimer pairs present in the structure of $[NBu^n_4][Rh(HL)(cod)]$ **1′**, showing also the C–H · · · O hydrogen bonding from the cation. Hydrogen-bonding geometries, X · · · O, H · · · O distances (Å) and X–H · · · O angles (°): *a*, 2.89(1), 2.00, 169; *b*, 3.28(1), 2.42, 149

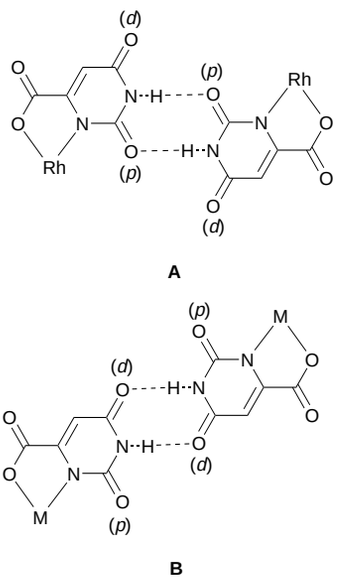

Scheme 2 Hydrogen-bonding modes observed in the crystal structures of complexes **1** (**A**) and **1′** and [Pt(HL)(dppe)] (**B**).[4a] Distal and proximal carbonyl functions are labelled (*d*) or (*p*) respectively

fashion *via* N–H · · · O hydrogen bonds (labelled *a* in Fig. 3) to produce discrete dimers as shown in Fig. 3.‡

The hydrogen-bonding mode in complex **1′** differs from that observed in **1** and **2** since it is the distal carbonyl oxygen atom O(4) which functions as the acceptor whereas in **1** and **2** the proximal carbonyl oxygen atom O(6) is utilised. In fact, the arrangement in **1′** is the same as that observed previously in the platinum orotate complexes [Pt(HL)(dppe)][4a] and [Pt(HL)-$(NH_3)_2$] (see Scheme 2).[4b] A possible reason for this apparent preference for the distal carbonyl oxygen atom to act as the acceptor in the dimer is that approach to the proximal carbonyl oxygen atom can be sterically hindered by the coligands at the metal centre. In **1**, **2** and **1′** the steric requirements of the cyclooctadiene ligand are not great and this permits both types of dimer formation to occur. Furthermore in **1** and **2** competition for the distal acceptor site is provided by the N–H group of the cation, a situation that does not arise in **1′**. There is evidence for a weak C–H · · · O hydrogen-bonding interaction between one of the cation methylene groups and the non-co-ordinated carboxylate oxygen atom (linkage *b* in Fig. 3).

‡ For the purpose of the hydrogen-bonding analyses, all the N–H and C–H bonds were normalised to 0.90 and 0.96 Å respectively.

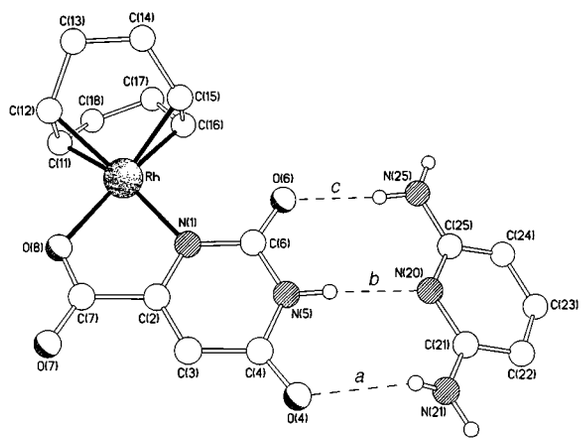

Fig. 4 Triple hydrogen bonding between $[Rh(HL)(cod)]^-$ and dap present in the structure of $[NBu^n_4][Rh(HL)(cod)]\cdot dap\cdot CH_2Cl_2$ **3**. Hydrogen-bonding geometries, N · · · X, H · · · X distances (Å) and N–H · · · X angles (°): *a*, 3.00(1), 2.33, 131; *b*, 3.04(1), 2.14, 175; *c*, 2.94(1), 2.08, 162

Synthesis and crystal structure of $[NBu^n_4][Rh(HL)(cod)]\cdot dap\cdot CH_2Cl_2$ 3

Slow evaporation of a dichloromethane solution containing equimolar quantities of rhodium complex **1′** and the complementary DAD base 2,6-diaminopyridine, dap, afforded yellow crystals of a new compound **3**. A crystal structure determination has confirmed formation of the adduct $[NBu^n_4][Rh(HL)(cod)]\cdot dap\cdot CH_2Cl_2$ **3** (see Fig. 4). Its packing is illustrated in Fig. 5.

The bond lengths and angles for the anion summarised in Table 1 differ little from those observed in the structures of complexes **1**, **2** and **1′**. Here the twist angle between the two co-ordination planes is *ca.* 4°. The dap unit engages in a DAD : ADA triple hydrogen-bonding interaction with the co-ordinated orotate ligand (linkages *a*, *b* and *c* in Fig. 4). In common with the previously characterised cocrystal [Pt(HL)-(dppe)]·dap,[4a] the substituted pyrimidine and dap rings are not coplanar, there being a fold angle of *ca.* 24° between them about an axis coincident with the N · · · N · · · N direction within the dap unit. The asymmetry of the two N–H · · · O hydrogen bonds of the DAD : ADA triple hydrogen bonding in the related platinum complex is not seen here, the N · · · O distances being 2.94(1) and 3.00(1) Å [*cf.* 3.04(1) and 2.88(1) Å]. This appears to be due to the fact that cod is less sterically demanding than dppe. In [Pt(HL)(dppe)]·dap there is steric repulsion between the phenyl groups of dppe and the proximal carbonyl function

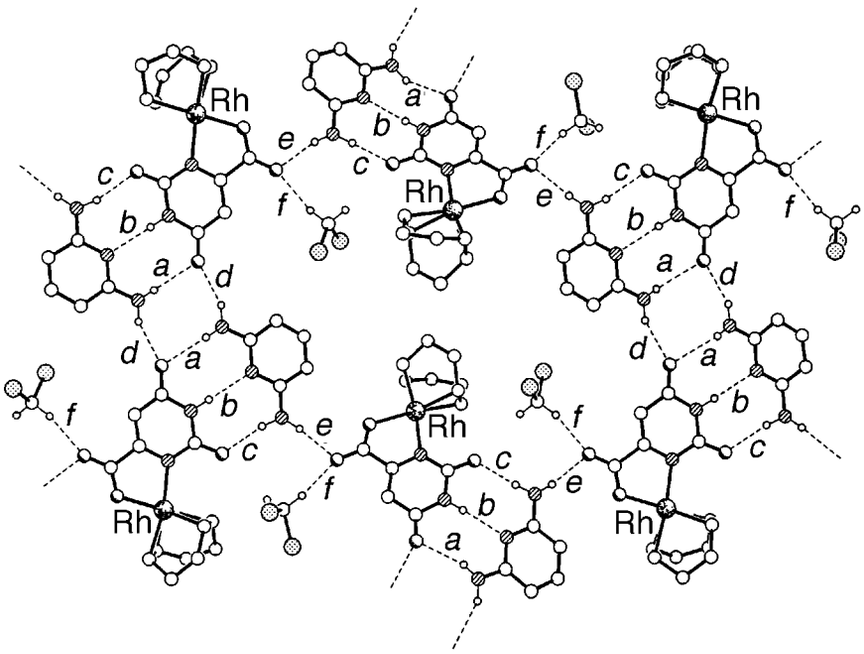

Fig. 5 Part of one of the extended hydrogen-bonded sheets comprised of 44-membered hydrogen-bonded rings present in the structure of $[NBu^n_4][Rh(HL)(cod)]\cdot dap\cdot CH_2Cl_2$ **3**. Hydrogen-bonding geometries, X · · · O, H · · · O distances (Å) and X–H · · · O angles (°): *d*, 2.95(1), 2.11, 154; *e*, 2.93(1), 2.05, 166; *f*, 3.12(1), 2.20, 162

of the orotate group which leads to the observed asymmetric hydrogen bonding to dap. A fundamental difference between the rhodium and platinum cocrystals is that the rhodium complex is negatively charged whereas the platinum species is neutral. Calculations on related metal-containing systems using density functional theory have suggested that the overall charge on a complex affects the strength of hydrogen bonds formed with complementary bases.[6] In a metal complex with an excess of carbonyl acceptors over N–H donors, a greater positive charge on the metal fragment leads to weaker hydrogen bonding with a complementary DAD molecule. We would thus expect stronger association to occur in the triply hydrogen-bonded dap adduct with $[Rh(HL)(cod)]^-$ than in the platinum compound. The two structural analyses, however, suggest that there is no overall statistically significant difference in the aggregated triple hydrogen-bond distances between the two species. It is likely that the differences due to charge are too small to be detected by the X-ray experiments.

The similarities between the structure of complex **3** and that reported previously for [Pt(HL)(dppe)]·dap extend to include the formation of centrosymmetric [2 + 2] 'dimers' *via* a pair of N–H · · · O hydrogen bonds involving one of the two amino hydrogen atoms not utilised in the triple hydrogen bonding in one molecule and the distal carbonyl oxygen atom in another and *vice versa* (link *d* in Fig. 5). The remaining amino hydrogen atom serves to link, through the non-co-ordinated carboxyl oxygen atom (bond *e* in Fig. 5), adjacent [2 + 2] dimer pairs to form slightly corrugated sheets of contiguous hydrogen-bonded adducts. In common with **1** and **2**, the included dichloromethane solvent molecules are involved in C–H · · · O hydrogen bonds to this same carboxyl oxygen atom (bond *f* in Fig. 5). In this structure, however, this hydrogen bond does not play an integral role in the creation of the extended hydrogen-bonded network, the contact to any potential acceptor site of the second CH_2Cl_2 hydrogen atom being too long for any significant interaction. The extended structure is in contrast to the discrete [2 + 2] adducts formed by [Pt(HL)(dppe)]·dap in the solid state, and again suggests that the steric effect of the coligand plays an important role in determining the degree of association in orotate complexes. The bulky phenyl groups of dppe are more effective than cod at blocking the carboxylate group and preventing it from acting as a hydrogen-bond acceptor.[4a]

Conclusion

This study has explored the effect of the metal and the coligands on the complementary hydrogen-bonding interactions between orotate complexes and diaminopyridine. The first examples of orotate complexes or rhodium and iridium have been synthesized and their structures examined. The structure of an adduct with diaminopyridine has also been established by single-crystal X-ray analysis. We have found that the steric bulk of the coligands plays an important role in shielding or allowing access to potential hydrogen-bonding sites, which affects the geometry and degree of aggregation of hydrogen-bonded adducts. The hydrogen-bonding abilities of the counter ions, solvent of crystallisation and coligand have all been shown to be important in influencing the observed hydrogen-bonding modes.

Experimental

Infrared spectra were recorded with a Perkin-Elmer 1720 FT spectrometer between 4000 and 250 cm^{-1} as KBr pellets, ^1H NMR spectra on a JEOL JNM-EX270 FT NMR spectrometer (^1H at 270 MHz) referenced internally to the ^1H impurity in the deuteriated solvent. Chemical shifts are reported in parts per million (ppm) relative to $SiMe_4$ (δ 0) using $(CD_3)_2SO$ (δ 2.52). Mass spectroscopy and microanalyses were carried out by the respective services provided by the Chemistry Department at Imperial College. Syntheses were conducted under dry nitrogen atmospheres using standard Schlenk techniques. Solvents were degassed, dried over appropriate agents and freshly distilled prior to use. The complexes $[M_2Cl_2(cod)_2]$ (M = Rh or Ir) were prepared according to the literature.[7] Orotic acid and 2,6-diaminopyridine were from Aldrich. 2,6-Diaminopyridine was recrystallised from chloroform prior to use.

Crystallography

Table 2 provides a summary of the crystal data, data collection and refinement parameters for compounds **1**, **2**, **1′** and **3**. Structures **1** and **3** were solved using the heavy-atom method, **2** and **1′** by direct methods; in each case all of the full-occupancy non-hydrogen atoms were refined anisotropically using full-matrix least squares based on F^2. In **1′** part of one of the butyl chains

Table 2 Crystal data, data collection and refinement parameters*

	1	**2**	**1′**	**3**
Formula	$C_{19}H_{30}N_3O_4Rh$	$C_{19}H_{30}IrN_3O_4$	$C_{29}H_{50}N_3O_4Rh$	$C_{29}H_{50}N_2O_4Rh{\cdot}C_5H_7N_3$
Solvent	CH_2Cl_2	CH_2Cl_2	—	CH_2Cl_2
M	552.3	641.6	607.6	801.7
Colour, habit	Yellow plates	Yellow prisms	Yellow needles	Yellow platy needles
Crystal size/mm	0.37 × 0.23 × 0.04	0.23 × 0.10 × 0.08	0.30 × 0.17 × 0.13	0.53 × 0.50 × 0.17
Lattice type	Monoclinic	Monoclinic	Tetragonal	Monoclinic
Space group	*C*2/*c* (no. 15)	*C*2/*c* (no. 15)	$I4_1/a$ (no. 88)	$P2_1/n$ (no. 14)
T/K	293	203	293	293
a/Å	16.005(1)	15.962(1)	20.273(1)	8.590(1)
b/Å	9.931(1)	9.881(1)	—	23.153(1)
c/Å	29.842(2)	29.685(1)	30.435(3)	20.750(1)
β/°	96.91(1)	96.83(1)	—	97.94(1)
U/Å^3	4708.8(5)	4648.6(4)	12 508(1)	4087.2(6)
Z	8	8	16	4
D_c/g cm^{-3}	1.558	1.833	1.291	1.303
F(000)	2272	2528	5152	1688
μ/mm^{-1}	8.21	13.50	4.69	4.92
θ Range/°	3.0–64.0	3.0–62.0	2.6–63.0	2.9–60.0
No. of unique reflections				
measured	3709	3649	5065	6046
observed, $\|F_o\|>4\sigma(\|F_o\|)$	2702	3063	3250	4038
Maximum, minimum transmission	0.77, 0.30	0.22, 0.09	0.48, 0.35	0.44, 0.15
No. variables	280	280	347	454
*R*1	0.057	0.042	0.062	0.061
*wR*2	0.131	0.104	0.130	0.138
Weighting factors *a*, *b*	0.084, 0.000	0.068, 10.069	0.050, 28.603	0.082, 0.316
Largest difference peak, hole/e Å^{-3}	0.63, −1.70	1.07, −0.90	0.48, −0.39	0.62, −0.47

* Details in common: graphite-monochromated Cu-Kα radiation (λ = 1.541 78 Å) (rotating-anode source for **2** and **1′**); ω scans; Siemens P4 diffractometer; semiempirical absorption correction; refinement based on F^2; $R1 = \Sigma\,||F_o| - |F_c||/\Sigma|F_o|$; $wR2 = [\Sigma w(F_o^2 - F_c^2)^2]/\Sigma w(F_o^2)^2]^{\frac{1}{2}}$; $w^{-1} = \sigma^2(F_o^2) + (aP)^2 + bP$.

of the counter ion was found to be disordered; this was resolved into two discrete, partial occupancy (60:40) orientations, the non-hydrogen atoms of the major occupancy orientation being refined anisotropically and those of the minor occupancy orientation isotropically. The C–H hydrogen atoms in all four structures were placed in calculated positions, assigned isotropic thermal parameters, $U(H) = 1.2U_{eq}(C)$ [$U(H) = 1.5U_{eq}$(C–Me)], and allowed to ride on their parent atoms. The N–H hydrogen atoms were located from Δ*F* maps and refined isotropically subject to a distance constraint. Computations were carried out using the SHELXTL PC program system.[8]

CCDC reference number 186/890.

See http://www.rsc.org/suppdata/dt/1998/1335/ for crystallographic files in .cif format.

Preparations

[NEt$_3$H][Rh(HL)(cod)]·CH$_2$Cl$_2$ 1. To a stirred solution of $[Rh_2Cl_2(cod)_2]$ (0.2 mmol) in CH_2Cl_2 (20 cm^3) was added orotic acid (254 mg, 1.46 mmol), Ag_2O (320 mg, 1.38 mmol) and NEt_3 (40 mg, 0.4 mmol). The mixture was refluxed for 3 h, cooled to room temperature and filtered. The filtrate was layered with hexane (20 cm^3) and left to stand to give the product as yellow rhombic crystals. Yield: 60% (Found: C, 45.47; H, 5.93; N, 8.04. $C_{19}H_{30}N_3O_4Rh{\cdot}0.5CH_2Cl_2$ requires C, 45.94; H, 6.13; N, 8.24%). IR (ν̃/cm^{-1}): 3135w (br), 3114w (br), ν(N–H); 1650s, 1631s, ν(C=O). Negative-ion FAB mass spectrum: *m*/*z* 365, $[Rh(C_8H_{12})(C_5H_2N_2O_4)]^-$. Positive-ion FAB mass spectrum: *m*/*z* 102, $[NEt_3H]^+$. ^{1}H NMR [$(CD_3)_2SO$]: δ 1.17 (CH_3, t, $^3J_{HH}$ = 7.3, 9 H), 1.67 (m, 4 H), 2.28 (m, 4 H), (cod CH_2, AA′BB′), 3.07 (CH_2, q, $^3J_{HH}$ = 7.3 Hz, 6 H), 4.25 (cod CH, s, 4 H), 5.75 (orotate CH, s, 1 H) and 9.92 (orotate NH, s, 1 H).

[NEt$_3$H][Ir(HL)(cod)]·CH$_2$Cl$_2$ 2. The synthesis was as for complex **1**, using $[Ir_2Cl_2(cod)_2]$ in place of $[Rh_2Cl_2(cod)_2]$, to give orange rhombic crystals. Yield: 68% (Found: C, 37.38; H, 4.93; N, 6.79. $C_{19}H_{30}IrN_3O_4{\cdot}CH_2Cl_2$ requires C, 37.44; H, 5.03; N, 6.55%). IR (ν̃/cm^{-1}): 3137w (br), 3107w (br), ν(N–H); 1660s, 1643s, ν(C=O). Negative-ion FAB mass spectrum: *m*/*z* 455, $[Ir(C_8H_{12})(C_5H_2N_2O_4)]^-$. Positive-ion FAB mass spectrum: *m*/*z* 102, $[NEt_3H]^+$. ^{1}H NMR [$(CD_3)_2SO$]: δ 1.13 (CH_3, t, $^3J_{HH}$ = 7.3, 9 H), 1.19 (m, 4 H), 2.06 (m, 4 H) (cod CH_2, AA′BB′), 3.07 (CH_2, q, $^3J_{HH}$ = 7.3 Hz, 6 H), 3.99 (cod CH, s, 4 H), 5.73 (orotate CH, s, 1 H) and 10.20 (orotate NH, s, 1 H).

[NBu$^n_4$][Rh(HL)(cod)] 1′. The complex $[Rh_2Cl_2(cod)_2]$ (246 mg, 0.5 mmol), orotic acid (210 mg, 1.2 mmol), Ag_2O (163 mg, 0.7 mmol) and NBu^n_4OH (1 M solution in methanol, 1 cm^3, 1 mmol) were stirred together in CH_2Cl_2 at room temperature for 4 h. The mixture was filtered, and diethyl ether (70 cm^3) added to the filtrate which was then left at −20 °C for 12 h. The resulting yellow crystals were collected at the pump, 383 mg, 63% (Found: C, 57.06; H, 8.04; N, 7.03. $C_{24}H_{50}N_3O_4Rh$ requires C, 57.32; H, 8.29; N, 6.92%). IR (ν̃/cm^{-1}): 3141w (br), ν(N–H); 1656s (br), ν(C=O). Negative-ion FAB mass spectrum: *m*/*z* 365, $[Rh(C_8H_{12})(C_5H_2N_2O_4)]^-$. Positive-ion FAB mass spectrum: *m*/*z* 242, $[NBu^n_4]^+$. ^{1}H NMR [$(CD_3)_2SO$]: δ 0.90 (CH_3, t, $^3J_{HH}$ = 7.2, 12 H), 1.13 (α-CH_2, m, 8 H), 1.29 (β-CH_2, m, 8 H), 1.63 (γ-CH_2, m, 8 H), 1.66 (m, 4 H), 2.28 (m, 4 H) (cod CH_2, AA′BB′), 3.06 (CH_2, t, $^3J_{HH}$ = 8.2 Hz, 6 H), 4.23 (cod CH, s, 4 H), 5.73 (orotate CH, s, 1 H) and 9.89 (orotate NH, s, 1 H).

[NBu$^n_4$][Rh(HL)(cod)]·dap·CH$_2$Cl$_2$ 3. The complex $[NBu^n_4]$-[Rh(HL)(cod)] (24.4 mg, 0.04 mmol) and dap (4.4 mg, 0.04 mmol) were dissolved in dichloromethane (5 cm^3). Slow evaporation yielded the product as yellow plates in <80% yield.

Acknowledgements

BP plc is thanked for endowing D. M. P. M.'s chair.

References

1 J. C. MacDonald and G. M. Whitesides, *Chem. Rev.*, 1994, **94**, 2383; C. B. Aakeroy and K. R. Seddon, *Chem. Soc. Rev.*, 1993, 397; G. R. Desiraju, *Chem. Commun.*, 1997, 1475.

2 A. D. Burrows, C.-W. Chan, M. M. Chowdhry, J. E. McGrady and D. M. P. Mingos, *Chem. Soc. Rev.*, 1995, 331; A. D. Burrows, D. M. P. Mingos, A. J. P. White and D. J. Williams, *J. Chem. Soc.*, *Dalton Trans.*, 1996, 3805; M. M. Chowdhry, D. M. P. Mingos, A. J. P. White and D. J. Williams, *Chem. Commun.*, 1996, 899; A. D. Burrows, D. M. P. Mingos, A. J. P. White and D. J. Williams, *Chem. Commun.*, 1996, 97; C.-W. Chan, D. M. P. Mingos, A. J. P. White and D. J. Williams, *Chem. Commun.*, 1996, 81; *Polyhedron*, 1996, **15**, 1753; J. D. Carr, L. Lambert, D. E. Hibbs, M. B. Hursthouse, K. M. A. Malik and J. H. R. Tucker, *Chem. Commun.*, 1997, 1649; N. Armaroli, F. Barigelletti, G. Calogero, L. Flamigni, C. M. White and M. D. Ward, *Chem. Commun.*, 1997, 2181; C. Price, M. R. J. Elsegood, W. Clegg, N. H. Rees and A. Houlton, *Angew. Chem.*, *Int. Ed. Engl.*, 1997, **36**, 1762; E. C. Constable and R.-A. Fallahpour, *J. Chem. Soc.*, *Dalton Trans.*, 1996, 2389; P. J. Davies, N. Veldman, D. M. Grove, A. L. Spek, B. T. G. Lutz and G. van Koten, *Angew. Chem.*, *Int. Ed. Engl.*, 1996, **35**, 1959; S. L. James, G. Verspui, A. L. Spek and G. van Koten, *Chem. Commun.*, 1996, 1309.

3 A. Karipides and B. Thomas, *Acta Crystallogr.*, *Sect. C*, 1986, **42**, 1705.

4 (*a*) A. D. Burrows, D. M. P. Mingos, A. J. P. White and D. J. Williams, *J. Chem. Soc.*, *Dalton Trans.*, 1996, 149; (*b*) T. Solin, K. Matsumoto and K. Fuwa, *Bull. Chem. Soc. Jpn.*, 1981, **54**, 3731.

5 M. C. Etter, *Acc. Chem. Res.*, 1990, **23**, 120.

6 J. E. McGrady and D. M. P. Mingos, *J. Chem. Soc.*, *Perkin Trans. 2*, 1996, 355.

7 J. L. Herde, J. C. Lambert and C. V. Senoff, *Inorg. Synth.*, 1974, **15**, 18; A. van der En and A. L. Onderdelinden, *Inorg. Synth.*, 1991, **28**, 90.

8 SHELXTL PC, version 5.03, Siemens Analytical X-Ray Instruments Inc., Madison, WI, 1994.

Received 14*th November* 1997; *Paper* 7/08205C